ABSTRACT
The abstract of the paper.

1 INTRODUCTION

1.1 Motivation

The fundamental parameters of stars, such as their effective temperatures and metallicities, dictate their observed apparent properties, such as their luminosities and spectra. Hence, a full accounting of the effects of these parameters, and any physical stellar processes that impact on them, directly or indirectly, must be sought.

1.2 Thermohaline mixing

The first months of the project were dedicated to the study of thermohaline mixing. This effect was proposed by ****Ulrich (1972) and ****Kippenhahn et al. (1982) to explain anomalous chemical abundances at the surface of mature (i.e post-first-dredge-up (FDU)), ****low-mass ($\lesssim$ red giant branch (RGB) stars. Specifically, the anomalies consist of an over-abundance of ^{12}C, ^{16}O and ^{14}N, together with a paucity of ^{7}Li and ^{1}H, in the stellar spectra. Taken together, these particular changes in these particular species indicate an interaction between the RGB star's fusion shell and the surface, i.e. a mixing effect. Thermohaline mixing is proposed as a solution to this problem in the post-FDU phase in low-mass ($< 1.5M_\odot$) RGB stars****.

Mixing of material occurs due to local thermodynamic instabilities. For stars, this requires consideration of 4 thermodynamic quantities: pressure P, temperature T, density ρ and molecular weight, μ, as well as a coordinate system in which to operate. For simple stellar models, radial symmetry is assumed, allowing the system to be reduced to the radial coordinate r, measured from the stellar centre. If we assume a fully-ionized plasma containing N atomic species, the local mean molecular weight can be calculated as:

$$\mu = \frac{1}{\sum_{i=1}^{i=N} (Z_i + 1)\frac{X_i}{A_i}}, \tag{1}$$

where, for each species i, Z_i is its proton number, A_i its atomic mass number and X_i its fraction by mass in the local region.

Most interior mixing in low-mass stars, including the FDU and main sequence phase mixing, occurs via convection. For convection of a bubble of material, of differing tempera chemical composition to its surroundings, to occur in a given stellar region, the local physical conditions, must satisfy the Schwarzschild criterion for instability:

$$\nabla_{\rm rad} > \nabla_{\rm ad} \tag{2}$$

where $\nabla_{\rm rad} = (\partial \ln T/\partial \ln P)_{\rm rad}$ and $\nabla_{\rm ad} = (\partial \ln T/\partial \ln P)_{\rm ad}$ are the temperature-pressure gradients for the local environment (dominated by radiation pressure) and the bubble (treated as an adiabatic ideal gas), respectively.

However, there is also the possibility of instability due to

The basic structure of low-mass RGB stars, starting from the physical centre of the star, can be summarised as follows:

(i) Inert, electron-degenerate ^{4}He-dominated core (98%

by mass), generally extending out to a coordinate fractional mass of $0.28M_\star$.

(ii) Fusion shell, in which the fusion reactions which previously occurred in the main-sequence core occur now in the RGB phase. The main reactions are the pp-chain and CNO cycle.

(iii) Radiative zone, consisting of layers for which the Schwarzschild criterion is NOT fulfilled, thus ensuring stability against convection. For a solar mass RGB star, this extends out to $0.29***M_\odot$, ****as calculated both in the model generated for this work by BaSTI and in (Eggleton et al. 2006), which, employed a fully-3D hydrodynamic approach.

(iv) Convective zone, where the Schwarzschild criterion is fulfilled, and mixing is modelled using the mixing-length theory (MLT), with the free parameter modelled such that, given solar input parameters, the model produces solar outputs.

(v) Atmosphere, where the radiation is emitted from the star - this layer consequently dominates the nature of the emission ($T_{\rm eff}$, emission lines, etc.)

^{3}He(^{3}He, 2^1H)^{4}He
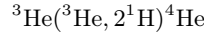
$$\frac{\partial X_i}{\partial t} = \frac{1}{\rho r^2} \frac{\partial}{\partial r} \left(\rho r^2 D \frac{\partial X_i}{\partial r} \right) \tag{3}$$

The strength of different diffusive effects in Equation 3 is dictated by their respective diffusion coefficient D. In the case of thermohaline mixing, the coefficient is defined Cantiello & Langer (2010) as:

$$D_{\rm thl} = C_{\rm thl} K \left(\frac{\phi}{\delta} \right) \frac{\nabla_\mu}{\nabla_{\rm rad} - \nabla_{\rm ad}} \tag{4}$$

where $C_{\rm thl}$ is a free parameter, which is set in this work to a value of $C_{\rm thl} = 1000$, $\nabla_\mu = d\ln\mu/d\ln P$, $\phi = (\partial \ln \rho/\partial \ln \mu)_{P,T}$, $\delta = -(\partial \ln \rho/\partial \ln T)_{P,\mu}$ (Kippenhahn et al. 1980) ****and K is the thermal diffusivity (Salaris & Cassisi 2017), defined as:

$$K = \frac{4acT^3}{3\kappa\rho^2 c_P} \tag{5}$$

where a is the radiation constant, c the speed of light, κ the Rosseland mean opacity and c_P the specific heat at constant pressure.

$$X_{i,n} = X_{i,n-1} + \delta t \left(\frac{\partial X_i}{\partial t} \right) \tag{6}$$

1.3 Differential extinction

Extinction of light between a source object, such as a star, and a remote observer is subject to various quantities, such as the density and metallicity of the interstellar medium along the emission travel path.

Bolometric corrections

After accounting for a general extinction effect on an object's emission, its apparent magnitude in a given filter X (i.e.

wavelength range, which we define as increasing from λ_1 to λ_2) is given by:

$$m_X = -2.5 \log_{10} \left(\frac{\int_{\lambda_1}^{\lambda_2} f_\lambda \left(10^{-0.4 A_\lambda} \right) S_\lambda d\lambda}{\int_{\lambda_1}^{\lambda_2} f_\lambda^0 S_\lambda d\lambda} \right) + m_X^0 \quad (7)$$

where f_λ represents the monochromatic flux at a given wavelength λ at the observer distance, A_λ is the extinction value as a function of wavelength, S_λ is the response function and f_λ^0 and m_X^0 represent the monochromatic flux and apparent magnitude, respectively, of a known reference object in X. In this project, the star Vega was used as the reference.

Since our goal, ultimately, is to document potential effects of fundamental stellar properties upon observables, we need to connect the observational and idealised scenarios, for which we use bolometric corrections. For a filter X, the extinction parameter A must be ****calibrated relative to a known value. For this reference, in this work we will input a value of the extinction in the well-studied Johnson-V filter. To derive the equation linking a bolometric correction with the extinction parameter, we start with the definition of a bolometric correction in X, BC_X:

$$BC_X \equiv M_{\text{bol}} - M_X \quad (8)$$

where M_X is the absolute magnitude of the object in X and M_{bol} is its (predicted) absolute bolometric magnitude, defined relative to the Sun using:

$$M_{\text{bol}} = M_{\text{bol},\odot} - 2.5 \log_{10} \left(\frac{4\pi R^2 F_{\text{bol}}}{L_\odot} \right) \quad (9)$$

where F_{bol} is the bolometric stellar flux at its surface, R is the stellar radius, $M_{\text{bol},\odot}$ is the solar absolute bolometric magnitude, ****which is assumed in this work to have a value of 4.75 and $L_\odot$ is the solar luminosity, for which we use a value of 3.844×10^{33} erg s^{-1} (****Girardi et al. (2000)). Bolometric corrections can be expressed as a function of extinction using the universal definition of M_X in terms of m_X and the distance d to the source:

$$M_X = m_X - 2.5 \log_{10} \left(\left(\frac{d}{10\text{pc}} \right)^2 \right), \quad (10)$$

together with the equation $f_\lambda d^2 = F_\lambda R^2$, where F_λ is the monochromatic flux at λ at the stellar surface. This gives the final function for a bolometric correction:

$$BC_X = M_{\text{bol},\odot} - m_X^0 - 2.5 \log_{10} \left(\frac{4\pi R^2 F_{\text{bol}}}{L_\odot} \right)$$
$$+ 2.5 \log_{10} \left(\frac{\int_{\lambda_1}^{\lambda_2} F_\lambda \left(10^{-0.4 A_\lambda} \right) S_\lambda d\lambda}{\int_{\lambda_1}^{\lambda_2} f_\lambda^0 S_\lambda d\lambda} \right) \quad (11)$$

To extract the extinction parameter A****, we use the simple relation:

$$A_X = \left(\frac{A_X}{A_V} \right) A_V \quad (12)$$

together with the chosen value of A_V (for this project the

values were $A_V = 0, 1$ - note that $BC_X(A_V = 0)$ effectively assumes no extinction), before taking the difference between the two $BC_X(A_V)$, giving the following equation:

$$BC_X(0) - BC_X(A_V) =$$
$$2.5 \log_{10} \left(\frac{\int_{\lambda_1}^{\lambda_2} F_\lambda S_\lambda d\lambda}{\int_{\lambda_1}^{\lambda_2} F_\lambda \left(10^{-0.4 \left(A_{X,\lambda}/A_V \right) A_V} \right) S_\lambda d\lambda} \right)$$
$$= \left(A_X/A_V \right) A_V \quad (13)$$

**** if $A_{X,\lambda}$ is assumed to constant within the wavelength range of each filter X, which is a valid assumption, even for the (wide-field) Hubble filters being studied in this work (Girardi****).
ATLAS9****

2 CURRENT STATE OF THE FIELD

2.1 Thermohaline mixing

Multiple**** studies have established the feasibility of thermohaline mixing in low-mass RGB stars from molecular mass gradient inversions as small as $(\delta\mu/\mu) \sim 10^{-4}$

2.2 Differential extinction

Many papers ****(such as ?) have examined the effects of extinction from multiple perspectives, many by examining ratios of reddening (a.k.a. colour excess) values as functions of wavelength primarily. The seminal work in this field is Cardelli et al. (1989), hereafter CCM, which avoided the complications of using reddening (which is not itself intrinsic and whose implications be impacted by the choice of filters) by fitting average ratios of the extinction parameter itself to observational data from stars taken in the IR, optical and UV spectral regions, as a**** function of wavelength λ. They produced a basic universal equation of the form:

$$A_\lambda/A_V = a(x) + b(x)/R_V, \quad (14)$$

where $x \equiv 1/\lambda$ and $R_V \equiv A(V)/E(B-V)$. The total wavelength range was divided into 4 subranges, each with a governing pair of empirically-determined equations (to determine $a(x)$ and $b(x)$, respectively). The CCM model underpins more recent studies of intrinsic effects on extinction (Casagrande & VandenBerg (2018), Girardi et al. (2008)), and provides the basis for the synthetic A_X/A_V dataset in this project.

ATLAS9 model atmosphere predictions, calculated for a given value of stellar metallicity Z and a grid of 476 combinations of T_{eff} and $\log(g)$ values (Castelli & Kurucz 2004) were used as synthetic stellar observation events

3 METHODOLOGY

For modelling thermohaline mixing, the BaSTI (Pietrinferni et al. (2004)) 1D full-star, full-lifespan stellar evolution code was used and modified to calculate the impact, on both the local radial layer and the overall star, of adding the effect

System	Filter	A_1 function	A_1 coefficients				
			a	σ_a	b	σ_b	c
WFC3	f218w	exp	cell1	cell2	cell3	cell1	cell2
	f225w	exp	cell4	cell5	cell6	cell1	cell2
	f275w	exp	cell7	cell8	cell9	cell1	cell2
	f300x	pow	cell7	cell8	cell9	cell1	cell2
	f336w	pow	cell7	cell8	cell9	cell1	cell2
	f390w	pow	cell7	cell8	cell9	cell1	cell2
	f438w	pow	cell7	cell8	cell9	cell1	cell2
	f475w	pow	cell7	cell8	cell9	cell1	cell2
	f555w	pow	cell7	cell8	cell9	cell1	cell2
	f606w	pow	cell7	cell8	cell9	cell1	cell2
	f625w	pow	cell7	cell8	cell9	cell1	cell2
	f775w	pow	cell7	cell8	cell9	cell1	cell2
	f814w	pow	cell7	cell8	cell9	cell1	cell2
Gaia	G	pow	cell7	cell8	cell9	cell1	cell2
	G_{bp}	pow	cell7	cell8	cell9	cell7	cell8
	G_{rp}	pow	cell7	cell8	cell9	cell7	cell8

of thermohaline mixing, on both short- and long-term time-scales.

When calculating the bolometric corrections, the reference values taken by the parameters for Vega were:

(i) $m_X^0 = 0.03$ for the Gaia filters
(ii) $m_X^0 = 0.00$ for the Hubble WFC3 filters

together with $M_{bol,\odot} = 4.75$. It should be noted that, during the final subtraction to obtain values of A_X/A_V, the m_X^0 and $M_{bol,\odot}$ values at both A_V calibration values are the same, so the final results are unaffected by any calibration errors.

4 RESULTS SO FAR

Initially, ****the values of A_X/A_V were fitted using a simple function of T_{eff} only, containing 3 free parameters, denoted by a, b and c. The results of this stage are stored in the function $A_1 = A_X/A_V(T_{eff})$. A_1 took on one of two function forms, depending on the relative performance of both in each filter. The first case, referred to in Table 4 by the abbreviation 'pow', models a fit of the following power-law form:

$$A_{1,pow}(T_{eff}) = a(T_{eff})^b + c \tag{15}$$

while the second case (denoted by 'exp') models an exponential:

$$A_{1,exp}(T_{eff}) = a\exp(bT_{eff}) + c \tag{16}$$

This first fitting step was carried out with ****no anchor points, for fixed values of stellar surface gravity ($\log(g/\text{cm s}^{-1}) = 5.0$) and metallicity ($Z = Z_\odot$). Due to a low-$T_{eff}$ artefact present in the data for several filters in both the WFC3 and Gaia systems, this project only analysed data for $T_{eff} \geq 4500$K.

As shown in Figure****, for some filters, there are significant changes in the extinction ratio values at fixed T_{eff} ($|\delta A| > 0.02$), due to changes in $\log(g)$, Z or both.

Castelli & Kurucz (2004)
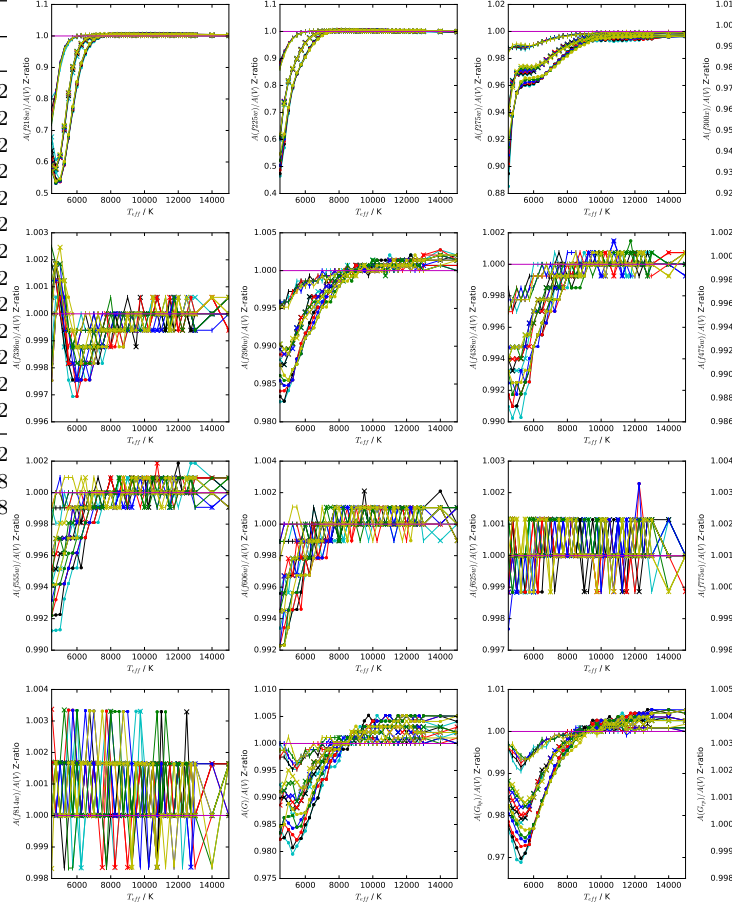
**Figure 1.** ****psrsoft image output for a simulated pulsar data file
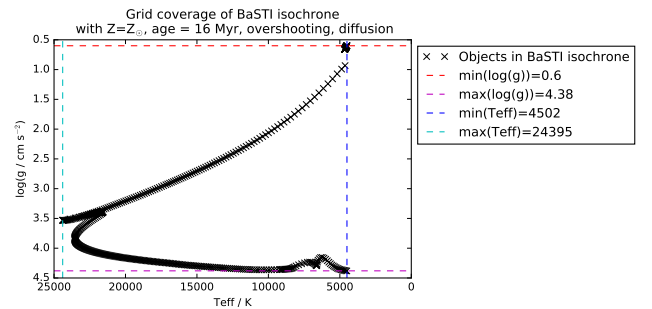
Figure 2. T_{eff}-$\log(g)$ grid coverage by a 16 Myr, $Z_\odot$ BaSTI isochrone ****including mass-loss, core overshooting and

5 DISCUSSION

5.1 Thermohaline mixing

As shown in Figure 4, the conditions for thermohaline mixing are reproduced in the BaSTI code. The location of the regions for which these conditions apply is located in the upper, and therefore cooler, layers of the hydrogen fusion shell,

So far, by measuring abundances of species which both are
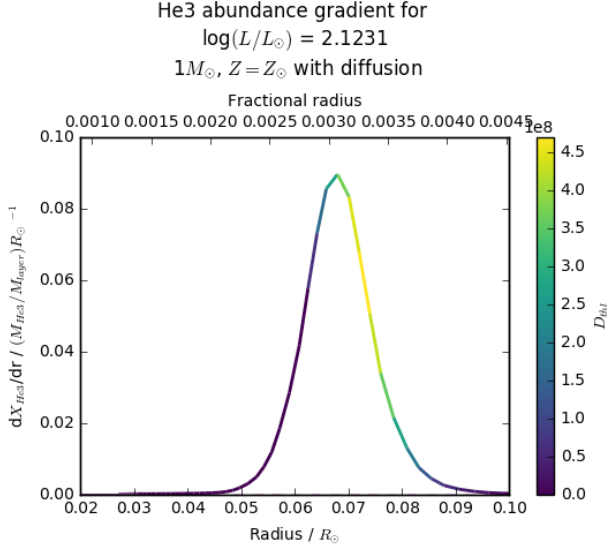
Figure 3. ^{3}He abundance gradient for model with $Z = Z_\odot$, $M = 1M_\odot$ and diffusion effects included, at a point $\log(L/L_\odot) = 2.1231$
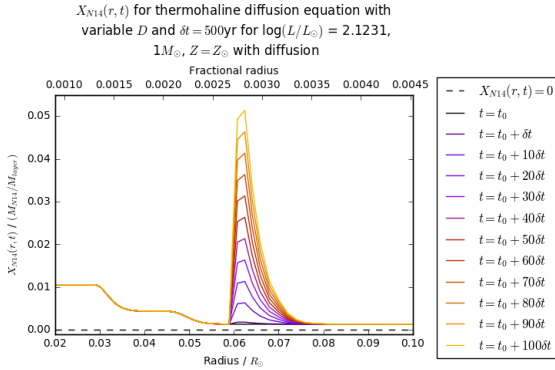
Figure 4. ^{14}N abundance time derivative for model with $Z = Z_\odot$, $M = 1M_\odot$ and diffusion effects included, at a point $\log(L/L_\odot) = 2.1231$

hydrogen fusion products and are not involved in ^{3}He burning, such as ^{14}N, it has been established that the existing BaSTI stellar evolution model creates the conditions for thermohaline mixing to occur in the radiative zone of a low-mass, post-FDU RGB star. It has also been shown that, as expected, the conditions are created by molecular weight inversions arising from ^{3}He burning.

While the physical process and impacts of thermohaline mixing have been successfully implemented in other stellar evolution codes, such as MESA and STAREVOL, BaSTI has not yet been modified to include these in the iterative calculations. Achieving this is a significant goal because, as demonstrated by Lattanzio et al. (2015) in the particular case of lithium abundances, there can be significant differences in predictions of abundances between different stellar evolution codes. Adding BaSTI to the list of codes available for future comparative studies would provide more scope to study potential sources of error, such as the model time-step

and C_{thl} value effects on abundances noted by Lattanzio et al. (2015). Of particular interest is the C_{thl} free-parameter value, as there are many proposed values, from authors using different approaches and models, which differ in some cases by at least an order of magnitude.

**** modelling/integrating other effects into BaSTI

5.2 Differential extinction

6 FUTURE WORK

This work, although confirming feasibility of thermohaline mixing in BaSTI, has yet to implement the effects of the resultant chemical mixing on the models of the star at times following the initial mixing.

References

Cantiello M., Langer N., 2010, A&A, 521, A9
Cardelli J. A., Clayton G. C., Mathis J. S., 1989, ApJ, 345, 245
Casagrande L., VandenBerg D. A., 2018, MNRAS, 479, L102
Castelli F., Kurucz R. L., 2004, ArXiv Astrophysics e-prints,
Eggleton P. P., Dearborn D. S. P., Lattanzio J. C., 2006, Science, 314, 1580
Girardi L., et al., 2008, PASP, 120, 583
Kippenhahn R., Ruschenplatt G., Thomas H.-C., 1980, A&A, 91, 175
Lattanzio J. C., Siess L., Church R. P., Angelou G., Stancliffe R. J., Doherty C. L., Stephen T., Campbell S. W., 2015, MNRAS, 446, 2673
Pietrinferni A., Cassisi S., Salaris M., Castelli F., 2004, ApJ, 612, 168
Salaris M., Cassisi S., 2017, Royal Society Open Science, 4, 170192